



Black String Bounce to Traversable Wormhole

Arthur Menezes Lima ¹, Geová Maciel de Alencar Filho ^{1,*}  and Job Saraiva Furtado Neto ² ¹ Departamento de Física, Universidade Federal do Ceará, Fortaleza 60455-760, Brazil² Departamento de Física, Universidade Federal do Cariri (UFCA), Av. Tenente Raimundo Rocha, Cidade Universitária, Juazeiro do Norte 63048-080, Brazil

* Correspondence: geova@fisica.ufc.br

Abstract: In this work, a regular black string solution is presented from the method used by Simpson–Visser to regularize the Schwarzschild solution. As in the Simpson–Visser work, in this new black string solution, it is possible to represent both a regular black hole and a wormhole simply by changing the value of a parameter “ a ” used in its metric. Tensors and curvature invariants are analyzed to verify the regularity of the solution as well as the energy conditions of the system. It is found that the null energy condition is always violated for the entire space. An additional analysis of the thermodynamic properties of the regular black string is carried out, in which the modifications generated about the original solution of the black string are evaluated, specifically, the Hawking temperature, entropy, its thermal capacity, and the Helmholtz free energy. Finally, we investigate the possible stable or unstable circular orbits for photons and massive particles. The results are compared with those for the non-regular black string, seeking to make a parallel with the Simpson–Visser work.

Keywords: black-bounce; Simpson-Visser; black string; black holes

1. Introduction

Black holes are solutions of Einstein’s equations in which there is the presence of a surface called the event horizon in which any matter or even light that passes through it can only describe a one-way path; not even light can travel off the horizon without violating causality [1]. This type of solution is very important in relativity, as it can define the type of geometry created when a body collapses, such as a star or star cluster [2]. These solutions have gained a great deal of relevance in recent years due to technological evolution, as evidenced by the detection of gravitational waves by LIGO and VIRGO and the first images of supermassive black holes [3–6].

In General Relativity, the main solutions for black holes form a family of four basic parameters called the generalized Kerr–Newman family. The four parameters are the mass M , angular momentum J , electric charge Q , and cosmological constant Λ . All these solutions have axial symmetry (i.e., they are axisymmetric), and can be asymptotically flat (when the cosmological constant is zero), *de Sitter* (if $\Lambda > 0$), or *anti-de Sitter* (if $\Lambda < 0$). As such, their asymptotic behavior depends directly on the cosmological constant [2]. A possible (though less common) solution is to consider cylindrical symmetry. This type of solution is particularly important for cosmology, as in the study of the evolution of the universe. In the phase transitions that may have occurred after the *big bang*, so-called topologically stable defects are studied, such as cosmic strings; these have generated very interesting results, such as density fluctuation, which explains the creation of galaxies [7]. These cosmic strings can be worked into cylindrical symmetry for spacetime. We call this the black string cylindrical black hole solution.

Basic black hole solutions to spacetime in General Relativity have a singularity at their origin, as matter collapses inwards. This is usually ignored, as there is not much physical interest in analyzing the origin of black holes. However, when working with black hole evaporation, these singularities cannot be ignored in the final stages of evaporation [8,9].



Citation: Lima, A.M.; de Alencar Filho, G.M.; Furtado Neto, J.S. Black String Bounce to Traversable Wormhole. *Symmetry* **2023**, *15*, 150. <https://doi.org/10.3390/sym15010150>

Academic Editor: Ghulam Mustafa

Received: 7 December 2022

Revised: 26 December 2022

Accepted: 28 December 2022

Published: 4 January 2023



Copyright: © 2023 by the authors. Licensee MDPI, Basel, Switzerland. This article is an open access article distributed under the terms and conditions of the Creative Commons Attribution (CC BY) license (<https://creativecommons.org/licenses/by/4.0/>).

However, it is possible to develop regular solutions for black holes. Spherically symmetric, static, asymptotically flat, and regular metrics can be found, including physically reasonable ones, without violating the energy conditions [10].

In this context, Simpson and Visser [11] proposed a regular solution through a modification of the Schwarzschild solution, presenting the following metric as a candidate to generate this solution:

$$ds^2 = -\left(1 - \frac{2m}{\sqrt{r^2 + a^2}}\right) dt^2 + \frac{dr^2}{\left(1 - \frac{2m}{\sqrt{r^2 + a^2}}\right)} + (r^2 + a^2) d\Omega^2, \quad (1)$$

where “ a ” represents an adjustable parameter and “ m ” is a constant that is related to the mass of matter that generates this curved spacetime. Essentially, the change $r^2 \rightarrow r^2 + a^2$ was carried out in the Schwarzschild solution. In summary, this metric has the following properties: if $a > 2m$, we have a two-way Morris–Thorne wormhole [11,12]; if $a = 2m$, we have a one-way wormhole with a horizon in the “throat”, similar to a Schwarzschild wormhole [11,12]; and if $a < 2m$, we have a regular one-way black hole with event horizons located at $r_H = \pm\sqrt{(2m)^2 - a^2}$ [11]. It is easy to see that the Schwarzschild solution is recovered when $a = 0$. After an analysis of the tensors and curvature invariants, it can be verified that there are no singularities at the origin, as $a \neq 0$. Another important fact is the violation of energy conditions due to the presence of matter to generate this solution, which occurs at any point in space-time and regardless of whether we have a black hole or a wormhole.

In addition, Simpson and Visser found expressions for the Hawking temperature of the regular solution and the circular orbits for photons (sphere of photons) and massive particles (ISCO), finding results similar to those of the Schwarzschild solution except with a correction factor of type $\sqrt{1 - a^2/k^2}$, where k is a constant multiple of m . In the case of temperature, $k = 2m$ [11]. It is possible to carry out a more in-depth analysis on the relationships between the Schwarzschild and Simpson–Visser solutions, such as the relationship between the degenerate shadows between them, through which both can generate the same shadow if their dominant photonspheres have the same impact parameter. The (spherically symmetric) shadow-degenerate geometries are divided into two classes, one of which corresponds to metrics with hypersurfaces having constant radius that are Schwarzschild isometric, which is exactly the case for the Simpson–Visser solution [13].

After the publication of their work, several others appeared along the same lines, treating already known non-regular solutions and performing Simpson–Visser regularization. Simpson himself published a work with the same regularization for Reisnerr–Nordstrom and Kerr–Newman black holes [14]; a thin disc accretion study for the Simpson–Visser solution can be found at [15], and this solution can be used to verify the impossibility of the existence of traversable wormholes in semiclassical gravitation [16]. In addition, there are works with modified gravity [17], gravitational lensing [18–20] (including use of the Gauss–Bonnet theorem to determine light deflection and analyze the effects of dark matter medium [21]), phantom fields [22,23], analysis of epicyclic oscillations [24], study of the quasinormal modes of the three states (black hole, wormhole, and one-way wormhole) of the Simpson–Visser solution [25,26], use of recent horizon scale images and their shadows (the Event Horizon Telescope image of Sagittarius A) to study several black hole solutions (including Simpson–Visser) [27], and the development of new more general black-bounce solutions exploiting changes in the metric [28].

However, until now there has been a gap in the literature regarding the regularization of the solution of a black string, which is the purpose of this work. The remainder of this work is organized as follows. In the following Section 2, we perform Simpson–Visser regularization on the metric obtained by Lemos in order to analyze whether any bounce from a black string to a wormhole occurs. In addition, we compute the tensors and curvature invariants in order to investigate their regularity. Moreover, we study the energy conditions of this solution. In Section 3, we perform an analysis of the thermodynamic properties and study

the possible circular orbits for photons and massive particles. Finally, in Section 4, we draw our conclusions.

2. Simpson-Visser Regularization for a Black String

First, let us briefly review the exact solution of a cylindrically symmetrical black hole with a negative cosmological constant in the context of general relativity, often called a black string. Thus, we are considering the coordinates $x^\mu = (t, r, \phi, z)$. These coordinates vary according to the following ranges: $t \in (-\infty, \infty)$; $r \in (-\infty, \infty)$; $\phi \in [0, 2\pi]$; $z \in (-\infty, \infty)$. For this type of solution, it is necessary to have a negative cosmological constant [2].

The ansatz for the metric is provided by

$$ds^2 = -f(r)dt^2 + \frac{dr^2}{f(r)} + r^2d\phi^2 + \alpha^2r^2dz^2, \tag{2}$$

where $\alpha^2 \equiv -\frac{1}{3}\Lambda > 0$ [2]. For our purposes, it is only necessary to use one component of the Einstein tensor, the component G^0_0 . Therefore, we obtain the following expression for G^0_0 :

$$G^0_0 = \frac{[f(r) + rf'(r)]}{r^2} = \frac{1}{r^2} \frac{d}{dr}[rf(r)], \tag{3}$$

where $f'(r) = df(r)/dr$. We are interested in the region where $r \neq 0$, which allows us to assume that in this region $T^0_0 = 0$. Thus, using Einstein's equation for G^0_0 and T^0_0 , we have

$$\frac{1}{r^2} \frac{d}{dr}[rf(r)] + \Lambda = 0, \tag{4}$$

for which the solution of $f(r)$ is provided by

$$f(r) = -\frac{\Lambda}{3}r^2 + \frac{C}{r}, \tag{5}$$

where C is a constant of integration. Following the usual solution defined in [2], we have

$$f(r) = \alpha^2r^2 - \frac{b}{\alpha r}. \tag{6}$$

The event horizon can be determined simply by setting $g_{00} = 0$

$$r \equiv r_{HL} = \frac{b^{1/3}}{\alpha}. \tag{7}$$

This solution is not regular, as the Kretschmann scalar $R^{\mu\nu\lambda\rho}R_{\mu\nu\lambda\rho} = 24\alpha^4\left(1 + \frac{b^2}{2\alpha^6r^6}\right)$ has a singularity at $r = 0$. Another interesting result is that the Ricci scalar is constant and proportional to the cosmological constant, specifically, $R = 4\Lambda = -12\alpha^2$, indicating that the curvature in the asymptotic limit is not zero. Therefore, the solution is not asymptotically flat.

Now, following the Simpson-Visser regularization scheme of the Schwarzschild metric, we seek to perform the same kind of regularization for the black string solution. In order to perform this regularization, we must consider the transformation $r \rightarrow \sqrt{r^2 + a^2}$ in the metric defined in (2), with $f(r)$ provided by (6), which yields

$$ds^2 = -\left(\alpha^2(r^2 + a^2) - \frac{b}{\alpha\sqrt{r^2 + a^2}}\right)dt^2 + \frac{dr^2}{\left(\alpha^2(r^2 + a^2) - \frac{b}{\alpha\sqrt{r^2 + a^2}}\right)} + (r^2 + a^2)[d\phi^2 + \alpha^2dz^2]. \tag{8}$$

For simplicity's sake, here we make another change to the radial coordinate: $\bar{r}^2 = r^2 + a^2$, a process similar to that in [13]. However, it should be noted that here we are not

changing the coordinates to return to the same Lemos solution; rather, we are making a coordinate change, which means that we now continue with the same solution defined in (8), which takes a simple and more intuitive form as

$$ds^2 = -\left(\alpha^2\bar{r}^2 - \frac{b}{\alpha\bar{r}}\right)dt^2 + \frac{d\bar{r}^2}{\left(1 - \frac{a^2}{\bar{r}^2}\right)\left(\alpha^2\bar{r}^2 - \frac{b}{\alpha\bar{r}}\right)} + \bar{r}^2d\phi^2 + \alpha^2\bar{r}^2dz^2. \tag{9}$$

The above metric can be rewritten as a function of the event horizon position $\bar{r}_H = b^{1/3}/\alpha$, meaning that

$$ds^2 = -\alpha^2\bar{r}^2\left(1 - \frac{\bar{r}_H^3}{\bar{r}^3}\right)dt^2 + \frac{d\bar{r}^2}{\alpha^2\bar{r}^2\left(1 - \frac{a^2}{\bar{r}^2}\right)\left(1 - \frac{\bar{r}_H^3}{\bar{r}^3}\right)} + \bar{r}^2d\phi^2 + \alpha^2\bar{r}^2dz^2. \tag{10}$$

Clearly, by setting $a = 0$ we recover the Lemos solution, which is not regular; thus, for our interest, we must assume $a \neq 0$. We can perform an analysis of null radial curves, which can be achieved by considering $ds^2 = d\phi = dz = 0$, leading to

$$\frac{d\bar{r}}{dt} = \pm\alpha^2\bar{r}^2\left(1 - \frac{\bar{r}_H^3}{\bar{r}^3}\right)\sqrt{1 - \frac{a^2}{\bar{r}^2}}. \tag{11}$$

As $\bar{r} = \pm\sqrt{r^2 + a^2}$, for $r = 0$ we have $\bar{r} = \pm a$; thus, a is the minimum value that the radial coordinate can have, similar to the “throat” of a wormhole. If $a > \bar{r}_H$, such as $\bar{r} \geq a$, the event horizon can never be reached, that is, the temporal term of the metric never vanishes, which implies that $d\bar{r}/dt$ is always non-zero except for $\bar{r} = a$ a value that is outside the event horizon. Therefore, this solution is characteristic of a traversable wormhole; however, such a wormhole is not of the Morris–Thorne type, as its symmetry is cylindrical rather than spherical. If $a = \bar{r}_H$, this means that in $\bar{r} = a$ there is an event horizon exactly at the “throat” of the wormhole, similar to the Simpson–Visser example. In this case, there is a one-way wormhole with an extreme “throat”. Finally, for $a < \bar{r}_H$, the event horizon can be reached at a value different from the minimum value a , as this has a value smaller than the horizon and the coordinate \bar{r} can assume any value greater than or equal to a . Consequently, as the coordinate moves away from the minimum value, that is, a itself, it approaches and reaches the horizon, indicating a black hole solution.

Now, we need to compute the tensors and the curvature invariants in order to analyze the regularity (or not) of these solutions and to finally study the Einstein equations and the energy conditions.

2.1. Tensors and Curvature Invariants

Our task now is to determine the Riemann and Ricci tensors, as well as the Ricci, Ricci contraction, and Kretschmann scalars, from the metric defined in Equation (10). The non-zero components of the Riemann tensor are

$$R^{01}_{01} = \frac{\alpha^2(2\bar{r}_H^3\bar{r}^2 - 3a^2\bar{r}_H^3 - 2\bar{r}^5)}{2\bar{r}^5}; \tag{12}$$

$$R^{02}_{02} = R^{03}_{03} = \frac{\alpha^2(a^2 - \bar{r}^2)(2\bar{r}^3 + \bar{r}_H^3)}{2\bar{r}^5}; \tag{13}$$

$$R^{12}_{12} = R^{13}_{13} = \frac{\alpha^2(3a^2\bar{r}_H^3 - \bar{r}_H^3\bar{r}^2 - 2\bar{r}^5)}{2\bar{r}^5}; \tag{14}$$

$$R^{23}_{23} = \frac{\alpha^2(a^2 - \bar{r}^2)(\bar{r}^3 - \bar{r}_H^3)}{\bar{r}^5}. \tag{15}$$

The non-zero components of the Ricci tensor can now be determined, and are provided by

$$R^0_0 = \frac{\alpha^2[a^2(4\bar{r}^3 - \bar{r}_H^3) - 6\bar{r}^5]}{2\bar{r}^5}; \tag{16}$$

$$R^1_1 = \frac{\alpha^2(3a^2\bar{r}_H^3 - 6\bar{r}^5)}{2\bar{r}^5}; \tag{17}$$

$$R^2_2 = R^3_3 = \frac{a^2\alpha^2}{\bar{r}^2} \left(\frac{\bar{r}_H^3}{\bar{r}^3} + 2 \right) - 3\alpha^2. \tag{18}$$

Adding all these components together, we can finally compute the Ricci scalar

$$R = -12\alpha^2 + \frac{3a^2\alpha^2(\bar{r}_H^3 + 2\bar{r}^3)}{\bar{r}^5}. \tag{19}$$

With the components of the Ricci tensor and Ricci scalar, we can determine the non-zero components of the Einstein tensor, which are

$$G^0_0 = \frac{\alpha^2[3\bar{r}^5 - a^2(\bar{r}^3 + 2\bar{r}_H^3)]}{\bar{r}^5}; \tag{20}$$

$$G^1_1 = \frac{3\alpha^2(\bar{r}^2 - a^2)}{\bar{r}^2}; \tag{21}$$

$$G^2_2 = G^3_3 = 3\alpha^2 - \frac{a^2\alpha^2}{\bar{r}^2} \left(\frac{\bar{r}_H^3}{2\bar{r}^3} + 1 \right). \tag{22}$$

Finally, the Ricci contraction and Kretschmann scalar are provided by

$$R^{\mu\nu}R_{\mu\nu} = 36\alpha^4 - \frac{18a^2\alpha^4(\bar{r}_H^3 + 2\bar{r}^3)}{\bar{r}^5} + \frac{3a^4\alpha^4(3\bar{r}_H^6 + 4\bar{r}_H^3\bar{r}^3 + 8\bar{r}^6)}{2\bar{r}^{10}}; \tag{23}$$

$$R^{\mu\nu\lambda\rho}R_{\mu\nu\lambda\rho} = \frac{12\alpha^4(\bar{r}_H^6 + 2\bar{r}^6)}{\bar{r}^6} + \frac{3\alpha^4[a^4(11\bar{r}_H^6 + 4\bar{r}^6) - 4a^2(3\bar{r}_H^6\bar{r}^2 + \bar{r}_H^3\bar{r}^5 + 2\bar{r}^8)]}{\bar{r}^{10}}. \tag{24}$$

Analyzing the components of the Riemann tensor and the scalars of curvature in the minimum value of \bar{r} , which is a , we obtain the following results:

$$R^{01}_{01} = -\frac{\alpha^2(\bar{r}_H^3 + 2a^3)}{2a^3}; R^{02}_{02} = R^{03}_{03} = R^{23}_{23} = 0; \tag{25}$$

$$R^{12}_{12} = R^{13}_{13} = \frac{\alpha^2(\bar{r}_H^3 - a^3)}{a^3}; \tag{26}$$

$$R = -12\alpha^2 + \frac{3\alpha^2(\bar{r}_H^3 + 2a^3)}{a^3}; \tag{27}$$

$$R^{\mu\nu}R_{\mu\nu} = 12\alpha^4 - \frac{12\alpha^4\bar{r}_H^3}{a^3} + \frac{9\alpha^4\bar{r}_H^6}{2a^6}; \tag{28}$$

$$R^{\mu\nu\lambda\rho}R_{\mu\nu\lambda\rho} = \frac{3\alpha^4(3\bar{r}_H^6 + 4a^6 - 4\bar{r}_H^3a^3)}{a^6}. \tag{29}$$

Therefore, as $a \neq 0$, it can be seen that there are no singularities in the curvature of this spacetime, that is, we have a regular solution for any non-zero parameter a . However, this solution is somewhat different from that found by Simpson–Visser, as its metric is not asymptotically flat, which can be seen when we carry out the same analysis with $|r| \rightarrow \infty$.

Because all the components of the Riemann tensor tend to $-\alpha^2$, the Ricci scalar tends to $-12\alpha^2$, the Ricci contraction to $36\alpha^4$, and the Kretschmann scalar to $24\alpha^4$, that is, within the asymptotic limit the curvature is not zero and depends on the cosmological constant.

2.2. Black String Momentum–Energy Tensor and Energy Conditions

We now discuss the energy conditions for a Simpson–Visser modified black string. We can define the pressures and energy density through the energy-momentum tensor, as follows:

$$T^0_0 = -\rho; T^1_1 = p_{\parallel}; T^2_2 = T^3_3 = p_{\perp}. \tag{30}$$

At first, we should define $T^2_2 = p_{\phi}$ and $T^3_3 = p_z$; however, because $G^2_2 = G^3_3$, we have $T^2_2 = T^3_3$.

Using Einstein’s equations with the cosmological constant, we can obtain the expressions for the components of the energy–momentum tensor as

$$\rho = \frac{\alpha^2 a^2 (\bar{r}^3 + 2\bar{r}_H^3)}{8\pi G \bar{r}^5}; \tag{31}$$

$$p_{\parallel} = -\frac{3\alpha^2 a^2}{8\pi G \bar{r}^2}; \tag{32}$$

$$p_{\perp} = -\frac{a^2 \alpha^2 (2\bar{r}^3 + \bar{r}_H^3)}{16\pi G \bar{r}^5}. \tag{33}$$

To assess whether this solution satisfies the energy conditions, in particular the null energy condition ($\rho + p_i \geq 0$), let us calculate $\rho + p_{\parallel}$

$$\rho + p_{\parallel} = -\frac{2a^2 \alpha^2 (\bar{r}^3 - \bar{r}_H^3)}{8\pi G \bar{r}^5}, \tag{34}$$

which is a valid result outside the event horizon, i.e., for $\bar{r} > \bar{r}_H$. It can be seen, therefore, that the right-hand-side of Equation (34) is always negative. This implies $\rho + p_{\parallel} < 0$, that is, that the null energy condition is violated, similar to the Simpson–Visser Schwarzschild case. Considering the region inside the event horizon, where $\bar{r} < \bar{r}_H$, we have to invert the space-like and time-like characteristics, which implies $T^0_0 = p_{\parallel}$ and $T^1_1 = -\rho$ [11]. Thus, for this region we have

$$\rho + p_{\parallel} = \frac{2a^2 \alpha^2 (\bar{r}^3 - \bar{r}_H^3)}{8\pi G \bar{r}^5}, \tag{35}$$

which in this case is again always negative, which implies that the null energy condition is violated in all cases. We can then generalize these results to both cases, i.e., inside and outside the event horizon, as follows:

$$\rho + p_{\parallel} = -\frac{2a^2 \alpha^2 |\bar{r}^3 - \bar{r}_H^3|}{8\pi G \bar{r}^5}. \tag{36}$$

The behaviour of the of the energy density, radial pressure, and $\rho + p_{\parallel}$ outside and inside the event horizon is depicted in Figures 1 and 2, respectively. The plots highlight that the null energy condition is always violated for the regions both outside and inside the event horizon.

It can be concluded that the regularization of the black string metric follows the same pattern as the regularization of the Schwarzschild solution found by Simpson–Visser. The Simpson–Visser modified black string solution can generate a wormhole or a black string depending on the parameter a used in the metric, and its solutions are all regular if $a \neq 0$. However, the energy conditions of the system are violated, that is, the type of regularization performed by Simpson–Visser results in violation of the system conditions, analogous to the case of Morris–Thorne wormholes [11,12].

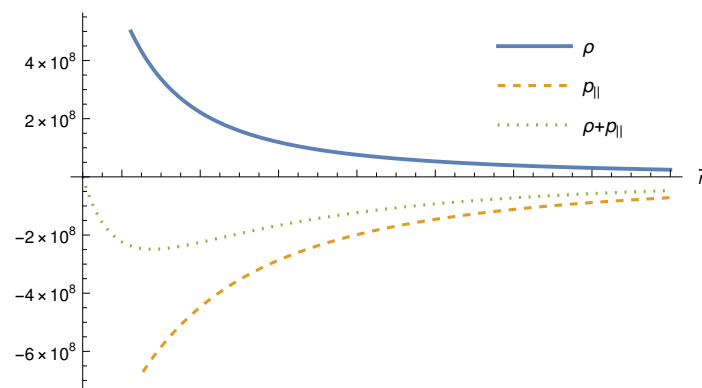


Figure 1. Energy density, radial pressure, and $\rho + p_{\parallel}$ outside the event horizon.

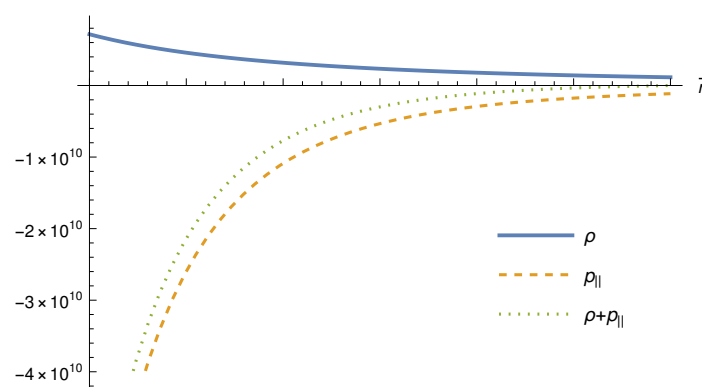


Figure 2. Energy density, radial pressure, and $\rho + p_{\parallel}$ inside the event horizon.

3. Applications of the Regular Solution of a Black String

Now, let us study the thermodynamic properties and the possible stable (or unstable) circular orbits for photons and massive particles. For such investigations, we must consider the metric in the form from (8). It is important to note that in this form the position of the event horizon is different, as g_{00} has another form. Defining this position by r_H , we have

$$r_H = \sqrt{r_{HL}^2 - a^2}, \quad (37)$$

where, as we have already seen, $r_{HL} = b^{1/3}/\alpha$.

3.1. Regular Black String Thermodynamics

The surface area bounded by the event horizon of a black hole always tends to increase or remain the same, giving rise to the Second Law of Black Holes. This is analogous to the Second Law of Thermodynamics for entropy, as the entropy of a given system of particles cannot decrease either, i.e., $\delta S \geq 0$. We might imagine that this is simple a coincidence or something superficial, as in the case of the area of a black hole this law has a mathematical rigor relative to General Relativity itself, while the second law of thermodynamics is not a law of nature, rather a consequence of the fact that in a physical system we are working statistically with a very large number of degrees of freedom. However, it is possible to find a parallel between the laws of black holes and the other laws of thermodynamics, showing that this relationship is indeed something fundamental and not merely a coincidence [29].

In light of these thermodynamic relationships associated with the magnitude of a black hole, we can then initially determine the temperature, known as the Hawking temperature, which can be expressed as follows:

$$T_H = \frac{\kappa}{2\pi} \quad (38)$$

where κ is the surface gravity, provided by $-g'_{00}(r_H)/2$ [30]. Thus, we have

$$T_H = \frac{3\alpha^2}{4\pi} \sqrt{r_{HL}^2 - a^2} = T_{HL} \sqrt{1 - \frac{a^2}{r_{HL}^2}}, \tag{39}$$

where $T_{HL} = 3\alpha^2 r_{HL} / (4\pi)$ is the solution temperature of the usual black string [31]. Here, the same pattern observed in [11] can be seen, that is, we have a correction factor in relation to the non-regular solution of the type $\sqrt{1 - a^2/k^2}$, where $k = r_{HL}$. It can be seen that for $a = 0$ we recover the usual black string solution, showing its consistency. When we have $a < r_{HL}$, the temperature tends to decrease with respect to T_{HL} , meaning that as $a \rightarrow r_{HL}$, T_H tends to zero, such as in the extreme throat wormhole case, where $a = r_{HL}$. For $a > r_{HL}$, the result obtained in (39) is no longer valid, which is reasonable, as in this interval we no longer have a black hole, but a wormhole with no event horizon.

For the sake of comparison, in Figure 3 we plot the behaviour of the Hawking temperature for three values of the bounce parameter a and the usual black string case. As can be seen, as we increase the value of the bounce parameter a we increase the value of r_{HL} in which the Hawking temperature vanishes. Furthermore, for large values of r_{HL} we recover the usual linear behaviour of the black string Hawking temperature.

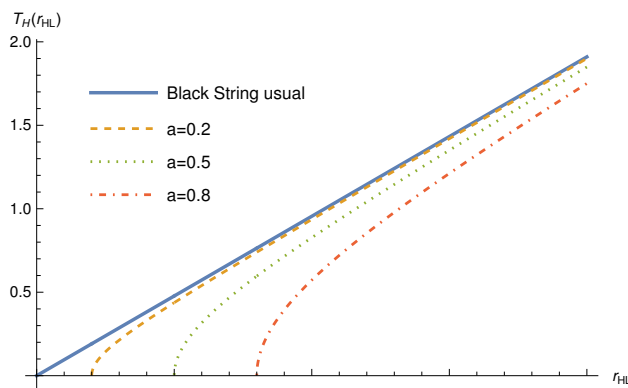


Figure 3. Hawking temperature.

Now, we can calculate the entropy and heat capacity, respectively, of the regular black string using the expressions $dS = dM/T$ and $C_V = dM/dT$ [30]. We can write the parameter b , defined in the black string metric, as $4M$ [32]. Thus, because $b = \alpha^3(r_H^2 + a^2)^{3/2}$, we have

$$dM = \frac{3}{4} \alpha^3 r_H \sqrt{r_H^2 + a^2} dr_H. \tag{40}$$

Now, we can write T_H as a function of r_H and integrate the expression dM/T to obtain the entropy as

$$S = S_L \left[\sqrt{1 - \frac{a^2}{r_{HL}^2}} + \frac{a^2}{r_{HL}^2} \ln \left(\frac{\sqrt{r_{HL}^2 - a^2} + r_{HL}}{a} \right) \right], \tag{41}$$

where $S_L = (\alpha/2)\pi r_{HL}^2$ is the entropy of the usual black string [31]. Here, it can be seen that the correction is not as trivial as in the case of the Hawking temperature, as in addition to the factor $\sqrt{1 - a^2/r_{HL}^2}$ we have a logarithmic function that depends on r_{HL} . First, we can see that the solution is consistent with the non-regular solution, because when $a \rightarrow 0$, the entropy tends to S_L . For $a < r_{HL}$, as a approaches r_{HL} the entropy value drops rapidly, such that at the limit $a \rightarrow r_{HL}$ the entropy drops to zero. For $a > r_{HL}$, the entropy value is not valid.

We can now calculate the heat capacity as

$$C_V = \frac{dM}{dr_H} \frac{dr_H}{dT} = \alpha\pi r_{HL} \sqrt{r_{HL}^2 - a^2} = C_{VL} \sqrt{1 - \frac{a^2}{r_{HL}^2}}, \tag{42}$$

where $C_{VL} = \alpha\pi r_{HL}^2$ is the value of the heat capacity of the usual black string [33]. It can be seen that it follows exactly the same pattern as the temperature, that is, we have the factor $\sqrt{1 - a^2/r_{HL}^2}$ correcting the usual value of the heat capacity; therefore, we can recover the usual result using $a = 0$, as expected. The sign of C_V is important to evaluate the thermodynamic stability of the black string, as if $C_V > 0$ this implies that the black hole is thermodynamically stable, and if $C_V < 0$ we have an unstable solution [31]. It can be seen in Equation (42) (and in Figure 4) that C_V is always positive, as is C_{VL} [33], indicating that this solution is always stable, with no possibility of evaporation, for example.

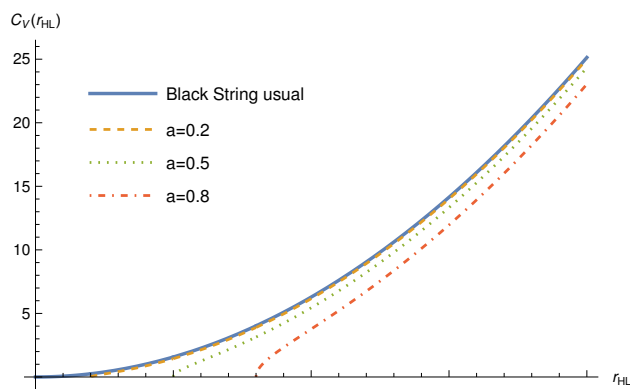


Figure 4. Heat capacity.

Finally, let us evaluate the Helmholtz free energy, provided by $F = M - T_H S$ [34]. Using the fact that $M = b/4$ together with Equations (39) and (41), we have

$$F = F_L \left(3\sqrt{1 - \frac{a^2}{r_{HL}^2}} \frac{S}{S_L} - 2 \right), \tag{43}$$

where $F_L = -\alpha^3 r_{HL}^3 / 8$ is the free energy of the usual solution. The result remains consistent, as when $a \rightarrow 0$, $S \rightarrow S_L$, and we retrieve the usual result F_L . Here, we again have a non-trivial dependence of the solution of F on a and r_{HL} , and when $a \rightarrow r_{HL}$, unlike the other quantities, F does not tends to zero, rather to $-2F_L$. Here, a pattern similar to that found in BTZ-type black hole regularization can be seen [34]; that is, when a is close to zero, the energy is negative, while when a approaches r_{HL} , the energy becomes positive. However, unlike [34], free energy is not allowed for $a > r_{HL}$.

3.2. Circular Orbits in the Regular Black String

One important result that we can find here is the possible circular orbits for this solution. A way to assess this is by determining the effective potential energy (V_{eff}) of the system formed by the black string and a massive particle or a photon. A stable orbit is one in which the concavity of the function is positive in the vicinity of the equilibrium point, that is, $V''_{eff} > 0$. For an unstable one, its concavity is negative, meaning that $V''_{eff} < 0$ [35].

For the sake of symmetry, we consider only the equatorial plane here, that is, $z = 0$. Thus, we have

$$\left(\frac{dr}{d\tau} \right)^2 = E^2 + \left(\alpha^2(r^2 + a^2) - \frac{b}{\alpha\sqrt{r^2 + a^2}} \right) \left(\epsilon - \frac{L^2}{r^2 + a^2} \right). \tag{44}$$

We can establish that

$$\left(\frac{dr}{d\tau} \right)^2 = E^2 - V_{eff}(r), \tag{45}$$

thus, by comparing Equation (44) with (45), we easily arrive at the expression for V_{eff} :

$$V_{eff}(r) = \alpha^2(r^2 + a^2) \left(1 - \frac{(r_H^2 + a^2)^{3/2}}{(r^2 + a^2)^{3/2}} \right) \left(\frac{L^2}{r^2 + a^2} - \epsilon \right). \tag{46}$$

The first case that we analyze is the circular path of light, by imposing $\epsilon = 0$ in (46) and using the condition $V'_{eff} = 0$. Therefore, we reach the following results:

$$V_{eff}(r) = \alpha^2 L^2 \left(1 - \frac{(r_H^2 + a^2)^{3/2}}{(r^2 + a^2)^{3/2}} \right); \tag{47}$$

$$V'_{eff}(r) = 3\alpha^2 L^2 r \left(\frac{(r_H^2 + a^2)^{3/2}}{(r^2 + a^2)^{5/2}} \right). \tag{48}$$

Here, it can be seen that the only possible solution for $V'_{eff}(r) = 0$ is $r = 0$. However, $r = 0$ implies $\bar{r} = a$, that is, either the light would be in the throat of a wormhole, as in the case of $a \geq r_{HL}$, or it would be inside the event horizon of a black hole, as in the case of $a < r_{HL}$. Therefore, this is clearly not a valid solution from a physical point of view [11]. As such, we can conclude that there are no circular orbits for a photon around a regular black string. The effective potential for massless particles is depicted in Figure 5.

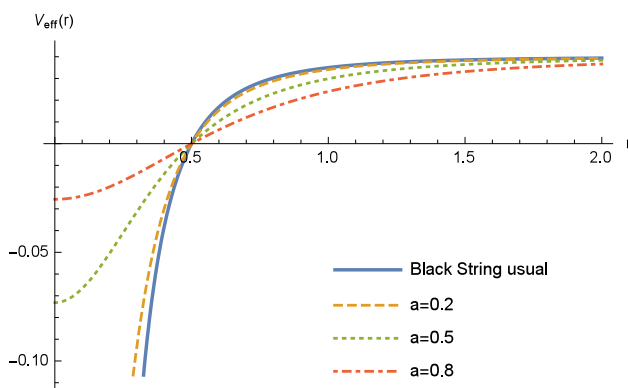


Figure 5. Effective potential for massless particles.

We now analyze the case of massive particles. Using the same reasoning as in the case of light, except now using $\epsilon = -1$, we have

$$V_{eff}(r) = \alpha^2 \left(1 - \frac{(r_H^2 + a^2)^{3/2}}{(r^2 + a^2)^{3/2}} \right) (L^2 + r^2 + a^2); \tag{49}$$

$$V'_{eff}(r) = \alpha^2 r \frac{3(L^2 + r^2 + a^2)(r_H^2 + a^2)^{3/2}}{(r^2 + a^2)^{5/2}} + 2\alpha^2 r \left(1 - \frac{(r_H^2 + a^2)^{3/2}}{(r^2 + a^2)^{3/2}} \right). \tag{50}$$

Imposing $V'_{eff}(r) = 0$, assuming $r \neq 0$, and setting L_c to be the angular momentum per unit mass of the circular orbit and r_c to be the radial coordinate value from the circular orbit, we can find L_c as a function of r_c , a , and r_H :

$$L_c^2 = - \left[\frac{(r_c^2 + a^2)}{3} + \frac{2(r_c^2 + a^2)^{5/2}}{3(r_H^2 + a^2)^{3/2}} \right]. \tag{51}$$

This expression cannot be physically valid, as the right side of Equation (51) is always negative for any r_c , a , and r_H . As a consequence, we would have complex angular momentum, which is not physically allowed. Therefore, there cannot be circular orbits for massive particles around a regular black string. These results are similar to the case of the regularization of a BTZ black hole [34], in which it is not possible to find circular orbits for either photons or massive particles. This indicates a similarity between the two types of solutions, and is quite different from the case analyzed by Simpson–Visser, in which orbits are found for both the photon sphere and massive particles. The effective potential for massive particles is depicted in Figure 6.

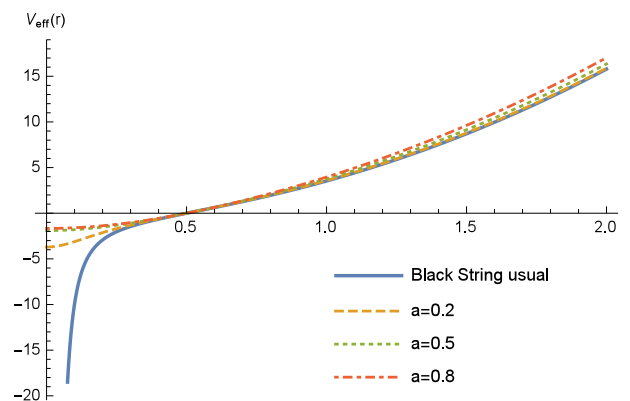


Figure 6. Effective potential for massive particles.

4. Conclusions

In this paper, we consider the solution of a black string already known in the literature and apply the same procedure employed by Simpson and Visser to regularize this solution. Thus, we obtain results similar to those found by Simpson and Visser, with interpolation between a regular black hole and a traversable wormhole, although this is not a Morris–Thorne wormhole. The regularity of the solution is verified by analyzing the tensors and curvature invariants, which are all finite at the origin because $a \neq 0$, where a is the parameter used to regularize the solution.

After determining the solution and verifying its regularity, an analysis of the energy conditions related to the moment-energy tensor is performed; again we identify the same pattern as in Simpson–Visser regularization, that is, the null energy condition is violated both inside and outside the event horizon for any kind of solution, whether regular black string or wormhole.

After this analysis of the curvature and energy conditions, we move on to basic applications of this solution. First, we analyze the thermodynamic properties of the black string. We verify that all the calculated quantities, namely, the Hawking temperature, entropy, heat capacity, and Helmholtz free energy, undergo change in relation to their usual respective values in the non-regular solution. In the case of the Hawking temperature and heat capacity, this change corresponds to the product of the usual value of the respective quantities with a correction factor of the type $\sqrt{1 - a^2/k^2}$, where $k = r_{HL} = b^{1/3}/\alpha$, which is the position of the event horizon in the usual solution. In the case of the entropy and Helmholtz energy the correction is more complex, involving both this factor and a logarithmic function. All quantities are consistent with the fact that the usual solution is recovered when $a \rightarrow 0$. At the limit where $a \rightarrow r_{HL}$, with the exception of the Helmholtz free energy, all quantities tend to zero. In the case of free energy, it changes from a negative value in the usual solution to a positive value as it approaches r_{HL} . In addition, we must highlight that the Simpson–Visser modification does not provide any change in the sign of the heat capacity, which is positive for any value of the bounce parameter a .

Finally, we analyze the possibilities of circular orbits for photons and massive particles. As a result, unlike the Simpson–Visser work, it is not possible to find circular orbits for the regular black string in any of the cases, as for both photons and massive particles the only

solution is found in $r = 0$, which is not physically reasonable as it would be inside the black hole or in the “throat” of the wormhole. Even if we were to find a value for the angular momentum that minimizes the circular orbit in the massive case, we find a negative value for L_c^2 , that is, we would have a complex angular momentum as a solution, which is not physically allowed.

As a future perspective, we intend to study the causal structure of this type of solution and to study the Simpson–Visser regularization of a black string with charge and angular momentum.

Author Contributions: Conceptualization, A.M.L., J.S.F.N. and G.M.d.A.F.; methodology, A.M.L., J.S.F.N. and G.M.d.A.F.; validation, A.M.L., J.S.F.N. and G.M.d.A.F.; formal analysis, A.M.L., J.S.F.N. and G.M.d.A.F.; investigation, A.M.L., J.S.F.N. and G.M.d.A.F.; writing—original draft preparation, A.M.L., J.S.F.N. and G.M.d.A.F.; writing—review and editing, A.M.L., J.S.F.N. and G.M.d.A.F.; visualization, A.M.L., J.S.F.N. and G.M.d.A.F.; funding acquisition, G.M.d.A.F. All authors have read and agreed to the published version of the manuscript.

Funding: This research was funded by Fundação Cearense de Apoio ao Desenvolvimento Científico e Tecnológico with grant number PRONEM PNE0112- 00085.01.00/16. National Council for Scientific and Technological Development with grant number N 315568/2021-6.

Institutional Review Board Statement: Not applicable.

Informed Consent Statement: Not applicable.

Data Availability Statement: Not applicable.

Acknowledgments: The authors would like to thank Conselho Nacional de Desenvolvimento Científico e Tecnológico (CNPq), Fundação Cearense de Apoio ao Desenvolvimento Científico e Tecnológico (FUNCAP), and Coordenação de Aperfeiçoamento de Pessoal de Nível Superior—Brasil (CAPES) for their financial support.

Conflicts of Interest: The authors declare no conflict of interest.

References

1. Visser, M. *Lorentzian Wormholes: From Einstein to Hawking*; AIP Press: New York, NY, USA, 1995.
2. Lemos, J.P.S. Cylindrical black hole in general relativity. *Phys. Lett. B* **1995**, *353*, 46–51. [[CrossRef](#)]
3. Akiyama, K.; Alberdi, A.; Alef, W.; Algaba, J.C.; Anantua, R.; Asada, K.; Azulay, R.; Bach, U.; Bacsko, A.K.; Ball, D.; et al. [Event Horizon Telescope]. First Sagittarius A* Event Horizon Telescope Results. I. The Shadow of the Supermassive Black Hole in the Center of the Milky Way. *Astrophys. J. Lett.* **2022**, *930*, L12.
4. Akiyama, K.; Alberdi, A.; Alef, W.; Asada, K.; Azuly, R. [Event Horizon Telescope]. First M87 Event Horizon Telescope Results. I. The Shadow of the Supermassive Black Hole. *Astrophys. J. Lett.* **2019**, *875*, L1.
5. Abbott, B.P.; et al. [LIGO Scientific and Virgo]. Observation of Gravitational Waves from a Binary Black Hole Merger. *Phys. Rev. Lett.* **2016**, *116*, 061102. [[CrossRef](#)]
6. Abbott, B.P.; et al. [LIGO Scientific and Virgo]. GW170817: Observation of Gravitational Waves from a Binary Neutron Star Inspiral. *Phys. Rev. Lett.* **2017**, *119*, 161101. [[CrossRef](#)] [[PubMed](#)]
7. Vilenkin, A. Cosmic Strings and Domain Walls. *Phys. Rept.* **1985**, *121*, 263–315. [[CrossRef](#)]
8. Carballo-Rubio, R.; Filippo, F.D.; Liberati, S.; Pacilio, C.; Visser, M. On the viability of regular black holes. *J. High Energy Phys.* **2018**, *07*, 023. [[CrossRef](#)]
9. Jayawiguna, B.N. Thermodynamics of regular Kerr-Sen black hole. *J. Phys. Conf. Ser.* **2022**, *2165*, 012016. [[CrossRef](#)]
10. Hayward, S.A. Formation and Evaporation of Nonsingular Black Holes. *Phys. Rev. Lett.* **2006**, *96*, 031103. [[CrossRef](#)]
11. Simpson, A.; Visser, M. Black-bounce to traversable wormhole. *J. Cosmol. Astropart. Phys.* **2019**, *2*, 42. [[CrossRef](#)]
12. Morris, M.S.; Thorne, K.S. Wormholes in space-time and their use for interstellar travel: A tool for teaching general relativity. *Am. J. Phys.* **1988**, *56*, 395–412. [[CrossRef](#)]
13. Lima, H.C.D.; Junior, Crispino, L.C.B.; Cunha, P.V.P.; Herdeiro, C.A.R. Can different black holes cast the same shadow? *Phys. Rev. D* **2021**, *103*, 084040. [[CrossRef](#)]
14. Simpson, A. From black-bounce to traversable wormhole, and beyond. *arXiv* **2021**, arXiv:2110.05657. [[CrossRef](#)]
15. Bambhaniya, P.; Jusufi, S.K.K.; Joshi, P.S. Thin accretion disk in the Simpson-Visser black-bounce and wormhole spacetimes. *Phys. Rev. D* **2022**, *105*, 023021.
16. Terno, D.R. Inaccessibility of traversable wormholes. *Phys. Rev. D* **2022**, *106*, 044035. [[CrossRef](#)]
17. Junior, E.L.B.; Rodrigues, M.E. Black-Bounce in $f(T)$ Gravity. *arXiv* **2022**, arXiv:2203.03629. [[CrossRef](#)]

18. Islam, S.U.; Kumar, J.; Ghosh, S.G. Strong gravitational lensing by rotating Simpson-Visser black holes. *J. Cosmol. Astropart. Phys.* **2021**, *10*, 013.
19. Nascimento, J.R.; Petrov, A.Y.; Porfirio, P.J.; Soares, A.R. Gravitational lensing in black-bounce spacetimes. *Phys. Rev. D* **2020**, *102*, 044021. [[CrossRef](#)]
20. Tsukamoto, N. Gravitational lensing in the Simpson-Visser black-bounce spacetime in a strong deflection limit. *Phys. Rev. D* **2021**, *103*, 024033. [[CrossRef](#)]
21. Övgün, A. Weak Deflection Angle of Black-bounce Traversable Wormholes Using Gauss-Bonnet Theorem in the Dark Matter Medium. *Turk. J. Phys.* **2020**, *44*, 465–471. [[CrossRef](#)]
22. Chataignier, L.; Kamenshchik, A.Y.; Tronconi, A.; Venturi, G. Regular black holes, universes without singularities, and phantom-scalar field transitions. *arXiv* **2022**, arXiv:2208.02280. [[CrossRef](#)]
23. Bronnikov, K.A. Black bounces, wormholes, and partly phantom scalar fields. *Phys. Rev. D* **2022**, *106*, 064029.
24. Stuchlík, Z.; Vrba, J. Epicyclic Oscillations around Simpson–Visser Regular Black Holes and Wormholes. *Universe* **2021**, *7*, 279. [[CrossRef](#)]
25. Churilova, M.S.; Stuchlik, Z. Ringing of the regular black-hole/wormhole transition. *Class. Quant. Grav.* **2020**, *37*, 075014. [[CrossRef](#)]
26. Yang, Y.; Liu, D.; Xu, Z.; Long, Z.W. Echoes from black bounces surrounded by the string cloud. *arXiv* **2022**, arXiv:2210.12641. [[CrossRef](#)]
27. Vagnozzi, S.; Roy, R.; Tsai, Y.D.; Visinelli, L.; Afrin, M.; Allahyari, A.; Bambhaniya, P.; Dey, D.; Ghosh, S.G.; Joshi, P.S.; et al. Horizon-scale tests of gravity theories and fundamental physics from the Event Horizon Telescope image of Sagittarius A*. *arXiv* **2022**, arXiv:2205.07787. [[CrossRef](#)]
28. Lobo, F.S.N.; Rodrigues, M.E.; Silva, M.V.d.S.; Simpson, A.; Visser, M. Novel black-bounce spacetimes: wormholes, regularity, energy conditions, and causal structure. *Phys. Rev. D* **2021**, *103*, 084052. [[CrossRef](#)]
29. Wald, R.M. *General Relativity*; The University of Chicago Press: Chicago, IL, USA, 1984. [[CrossRef](#)]
30. Alencar, G.; Muniz, C.R. Thermodynamic Properties of Static and Rotating Unparticle Black Holes. *J. Cosmol. Astropart. Phys.* **2018**, *3*, 040. [[CrossRef](#)]
31. Carvalho, I.D.D.; Furtado, J.; Landim, R.R.; Alencar, G. Horizon Fractalization in Black Strings Ungravity. *arXiv* **2022**, arXiv:2209.14793.
32. Rayimbaev, J.; Demyanova, A.; Camci, U.; Abdujabbarov, A.; Ahmedov, B. Dynamics of charged and magnetized particles around cylindrical black holes immersed in external magnetic field. *Int. J. Mod. Phys. D* **2021**, *30*, 2150019.
33. Nilton, M.; Alencar, G. Black Strings in Asymptotically Safe Gravity. *arXiv* **2022**, arXiv:2211.02581. [[CrossRef](#)]
34. Furtado, J.; Alencar, G. BTZ Black-bounce to Traversable Wormhole. *arXiv* **2022**, arXiv:2210.06608.
35. Jefremov, P.I.; Tsupko, O.Y.; Bisnovatyi-Kogan, G.S. Innermost stable circular orbits of spinning test particles in Schwarzschild and Kerr space-times. *Phys. Rev. D* **2015**, *91*, 124030. [[CrossRef](#)]

Disclaimer/Publisher’s Note: The statements, opinions and data contained in all publications are solely those of the individual author(s) and contributor(s) and not of MDPI and/or the editor(s). MDPI and/or the editor(s) disclaim responsibility for any injury to people or property resulting from any ideas, methods, instructions or products referred to in the content.